Ma *et al. Clinical Epigenetics* (2026) 18:45
https://doi.org/10.1186/s13148-026-02060-w

Clinical Epigenetics

RESEARCH Open Access

Trimethylamine N-oxide and related metabolites may regulate DNA methylation and trigger cardiovascular disease

Jiantao Ma[1†], Chao-Qiang Lai[2†], Xinmin S. Li[3], Meng Wang[1], Zeneng Wang[3], Jie Yao[4], Xiuqing Guo[4], Kent D. Taylor[4], Soyoung Lee[1], Russell P. Tracy[5], Durda Peter[5], Yongmei Liu[6], Jerome I. Rotter[4], Stephen S. Rich[7], Matthew Budoff[8], WHWilson Tang[3,9], Joseph A. DiDonato[3], Jennifer A. Brody[10], Rozenn N. Lemaitre[10], Amanda Fretts[10], Nona Sotoodehnia[10], Bruce M. Psaty[11], José M. Ordovás[12], David S. Siscovick[13], Stanley L. Hazen[3,9] and Dariush Mozaffarian[1*]

Abstract

Background Trimethylamine N-oxide (TMAO) and its related metabolites have been linked to cardiovascular disease (CVD), but their impact on DNA methylation remains unclear. Investigating these relationships may clarify the role of epigenetic mechanisms in diseases.

Methods This study analyzed data from 1,356 adults from the Cardiovascular Health Study (CHS) and the Multi-Ethnic Study of Atherosclerosis (MESA). Using stable-isotope dilution liquid chromatography with on-line electrospray ionization tandem mass spectrometry (LC–MS), we quantified TMAO and five related metabolites. DNA methylation levels were measured using Illumina BeadChip arrays. Epigenome-wide association analyses and meta-analyses were conducted across approximately 430,000 CpG sites. To explore the functional significance of the identified CpGs, we performed gene set enrichment analysis and Mendelian randomization (MR) analyses.

Results We identified 143 metabolite-CpG pairs at FDR < 0.05, including four CpGs for TMAO (P ≤ 4.03e-7), 12 for betaine (P ≤ 1.19e-6), 53 for γ-butyrobetaine (P ≤ 6.11e-6), five for carnitine (P ≤ 5.42e-7), six for choline (P ≤ 2.81e-7), and 63 for crotonobetaine (P ≤ 7.25e-6). CpGs associated with γ-butyrobetaine showed moderate correlation with crotonobetaine-associated CpGs. In total, these metabolite-linked CpGs were mapped to 108 genes. Gene set enrichment analysis revealed 145 significantly enriched gene sets, including nine highly relevant to CVD risk. Furthermore, CpGs were enriched in 80 immunologic signature gene sets (FDR < 0.05). MR analysis identified three CpGs associated with coronary artery disease (CAD), including hypermethylation at cg18705301 (*NDUFAF1*), which was inversely associated with betaine levels and linked to a lower risk of CAD (P = 1.8e-5).

†Jiantao Ma and Chao-Qiang Lai These authors contributed equally to this work.

*Correspondence:
Dariush Mozaffarian
Dariush.Mozaffarian@tufts.edu

Full list of author information is available at the end of the article

Conclusion This study identified specific DNA methylation sites associated with TMAO and related metabolites. These epigenetic changes may contribute to CVD risk through multiple pathways. Future research should validate these findings and explore their clinical implications.

Introduction

A higher intake of meat, particularly unprocessed red meat, was associated with increased incidence of atherosclerotic CVD [1]. Red meat and other animal source foods such as egg yolk, pork, and liver are rich in choline, phosphatidylcholine, and L-carnitine. These nutrients are also broadly consumed as dietary supplements. Gut microbes can process these nutrients to produce trimethylamine (TMA), which is subsequently converted to trimethylamine-N-oxide (TMAO) in the liver [2, 3]. A higher level of TMAO in circulation has been associated with a greater risk of cardiovascular disease (CVD). Findings from our previous study, coupled with numerous animal model and mechanistic studies [2–6], support a potential mechanism by which gut microbiota-derived metabolites may link diet to atherosclerotic CVD.

Current evidence suggests that TMAO may influence CVD and CVD comorbidity and underlying disease processes [7–10]. TMAO has been shown to alter cholesterol metabolism, leading to an increased cholesterol deposits in the arterial walls [3, 11]. It has also been implicated in promoting inflammation, a known risk factor for atherosclerosis [12–14]. Additionally, TMAO can induce endothelial cell activation and dysfunction, impairing the ability of blood vessels to dilate properly and maintain healthy blood flow [14, 15]. TMAO also induces platelet activation [4, 16–18], which may lead to the formation of clots that obstruct blood flow and cause heart attack or stroke. Despite these findings, and the ability to modulate CVD-relevant phenotypes in animal models by manipulating TMAO levels in vivo by multiple mechanisms, there remain numerous questions as to how TMAO and/or TMAO-related metabolites modulate CVD risk, and translation of therapeutic interventions into human studies has not yet occurred.

Similar to TMAO and TMAO-related metabolites, DNA methylation levels can be affected by lifestyle factors such as diet. DNA methylation is the most highly studied epigenetic modification. Differential DNA methylation at over one thousand CpGs (i.e., DNA methylation sites) has been associated with CVD [19–25]. Several studies have explored the impact of gut microbial choline and TMAO metabolism on DNA methylation profiles. For example, early studies by Romano and colleagues demonstrated that mice harboring high levels of choline-consuming bacteria showed increased susceptibility to metabolic disease in the context of increased TMAO generation on a high-fat diet; moreover, alterations in gut microbiome capacity to transform choline into TMA, the rate-limiting step in metaorganismal TMAO generation, were shown to influence global DNA methylation patterns in both adult mice and their offspring, while simultaneously also inducing TMAO-dependent changes in behavior [26].

In a study of 283 middle-aged to older adults, higher plasma TMAO levels were associated with a lower methylation potential, reflecting reduced levels of S-adenosylhomocysteine and S-adenosylmethionine [27]. TMAO-related metabolites such as betaine and choline—both dietary substrates for TMAO generation—are key factors in the one-carbon metabolism that can alter methyl source and affect DNA methylation status [28]. One study examined the relationship between TMAO levels, measured using proton nuclear magnetic resonance (NMR) spectroscopy, and DNA methylation in CD4 + T-cells in 847 adults [29]. This epigenome-wide association study (EWAS) identified a few candidates, but no CpGs reached statistical significance after correction for multiple testing. In the present study, we increased the sample size to boost statistical power for CpG identification. More importantly, relative to the semiquantitative approach used in the previous TMAO-EWAS study, we used a robust approach to quantify metabolite concentrations. This approach reduced measurement errors; therefore, the present study further improved statistical power. In addition, we expanded the previous EWAS by including TMAO and five TMAO-related metabolites, including (choline, betaine, carnitine, γ-butyrobetaine, and crotonobetaine).

Methods

Study design and population

We analyzed data from participants from the CHS and the Multi-Ethnic Study of Atherosclerosis (MESA), two well-established, multi-center, community-based prospective cohort studies [30, 31]. Additional methodological details are provided in the Supplementary Methods. Briefly, in CHS, 5,201 noninstitutionalized predominantly White adults aged ≥ 65 years were recruited from random samples of Medicare eligibility lists in four US communities from 1989 to 1990. From 1992 to 1993, an additional 687 Black participants were recruited, resulting in 5,888 total participants. In MESA, 6,814 adults aged 45–84 years were recruited from six study sites between 2000 and 2002; participants were 38% White, 28% Black, 22% Hispanic, and 12% Chinese-American participants. A total of 5,019 CHS participants and 6,796 MESA participants had TMAO measures at baseline

from an ancillary study on cardiovascular risk, and we had epigenetic data from 665 CHS and 937 MESA participants, resulting in 430 CHS participants and 926 MESA participants with both measures in the final analysis. The study was approved by the Tufts Institutional Review Board. All participants provided written informed consent, and all research was conducted in accordance with the Declaration of Helsinki.

Measurement of TMAO and related metabolites

Plasma samples were analyzed for TMAO and related metabolites (choline, betaine, carnitine, γ-butyrobetaine, and crotonobetaine) as previously described [32]. Briefly, frozen (-80 °C) fasting blood samples collected 1989–1993 in CHS and 2000–2002 in MESA were used. Each metabolite and its deuterium-isotopologue (internal standard) were quantified using a stable-isotope dilution assay coupled with high-performance liquid chromatography, with online electrospray ionization tandem mass spectrometry on a Shimadzu 8050 or 8060 mass spectrometer, as previously described [1, 33]. All six metabolites had laboratory coefficient of variation < 10%. Natural log transformation was applied before formal statistical analysis.

DNA methylation assessment

Methylation levels were measured on whole blood derived DNA samples collected during the 1994–1995 visit in CHS and the 2000–2002 exam in MESA [34, 35]. Illumina HumanMethylation450 BeadChip array (450 K array) was used in CHS, whereas Illumina MethylationEPIC BeadChip array (EPIC array) was used in MESA. The 450 K array targets 485,512 CpGs and the EPIC array targets 866,836 CpGs; ~ 93% of CpGs in the 450 K array are covered by the EPIC array [36]. We primarily analyzed CpGs that are common to both arrays. Cohort-specific quality control and normalization had been performed following standard protocols. In CHS, the *minfi* R package was used for DNA methylation quality control (QC) [37, 38]. Samples were excluded if median intensities across the methylated and unmethylated changes were < 10.5 (log 2), > 0.5% of probes failed detection, QC probes fell > 3 SD from the mean, or sample swaps were likely due to sex mismatches or genotype inconsistency with prior genotyping. Subset-quantile Within Array Normalization (SWAN) was implemented to standardize DNA methylation values [39]. In MESA, participant samples were excluded based on poor detection ability in more than 5% of CpG measurements, intensity values less than three standard deviations below the mean, or sex mismatched. Methylation profiles were preprocessed using background and dye-bias correction using RELIC in the Enmix [40, 41], inter-array (quantile) normalization [40], and probetype bias correction using *Rcp* in the Enmix [42] R package. We also excluded probes on the X and Y chromosomes to avoid potential sex bias. The methylation level at each CpG was quantified as a β value, i.e., the proportion of methylated CpGs over the sum of methylated and unmethylated CpGs.

Covariates

In both cohorts, sociodemographic factors (e.g., age, sex, race/ethnicity, household income, and education), anthropometric factors (e.g., body weight and height), and medication use (e.g., antibiotics; typically within 2 weeks) were assessed by trained staff using cohort-specific questionnaires during participants' physical examinations [30, 31]. BMI was calculated using weight in kilograms divided by the square of height in meters. Dietary habits over the past year were measured using cohort-specific semi-quantitative food frequency questionnaire (FFQ) [43, 44]. A DASH (dietary approach to stop hypertension) diet score was calculated to reflect diet quality in CHS [45], whereas the AHEI (Alternative Healthy Eating Index) score was used in MESA [46]. Algorithms for calculating the AHEI and DASH scores have been described previously [47–49]. Physical activity was assessed using validated, cohort-specific semi-quantitative questionnaires that capture frequency and duration of various physical activities [50, 51]. Alcohol consumption and smoking status (never, former, and current smoker) were also collected during physical exams. Estimated glomerular filtration rate (eGFR) was calculated using the Chronic Kidney Disease Epidemiology Collaboration (CKD-EPI) creatinine–cystatin C equation [52]. We used the covariates collected from the 1989–1990/1992–1993 CHS exams and the 2000–2002 MESA exam.

Statistical analysis

Our study design was depicted in Fig. 1. We first conducted EWAS using linear regression models with DNA methylation levels as dependent variables and TMAO and TMAO-related metabolites as independent variables. Metabolite concentrations were standardized to mean of 0 and standard deviation of 1 before EWAS. We examined these metabolites in separate models, i.e., each model examined association of a single metabolite with a single CpG. Three sets of covariates were included: 1) sex, age, study site, blood cells composition (estimated using the Houseman method [53]), technical variables (i.e., to control cohort-specific batch effects), education level, household income, and recent antibiotic use, 2) smoking status (none, former, current), alcohol intake, physical activity, and diet quality scores, and 3) BMI and eGFR. The association was analyzed in each race/ethnicity group, and to account for the racial and ethnic differences in DNA methylation patterns, we used

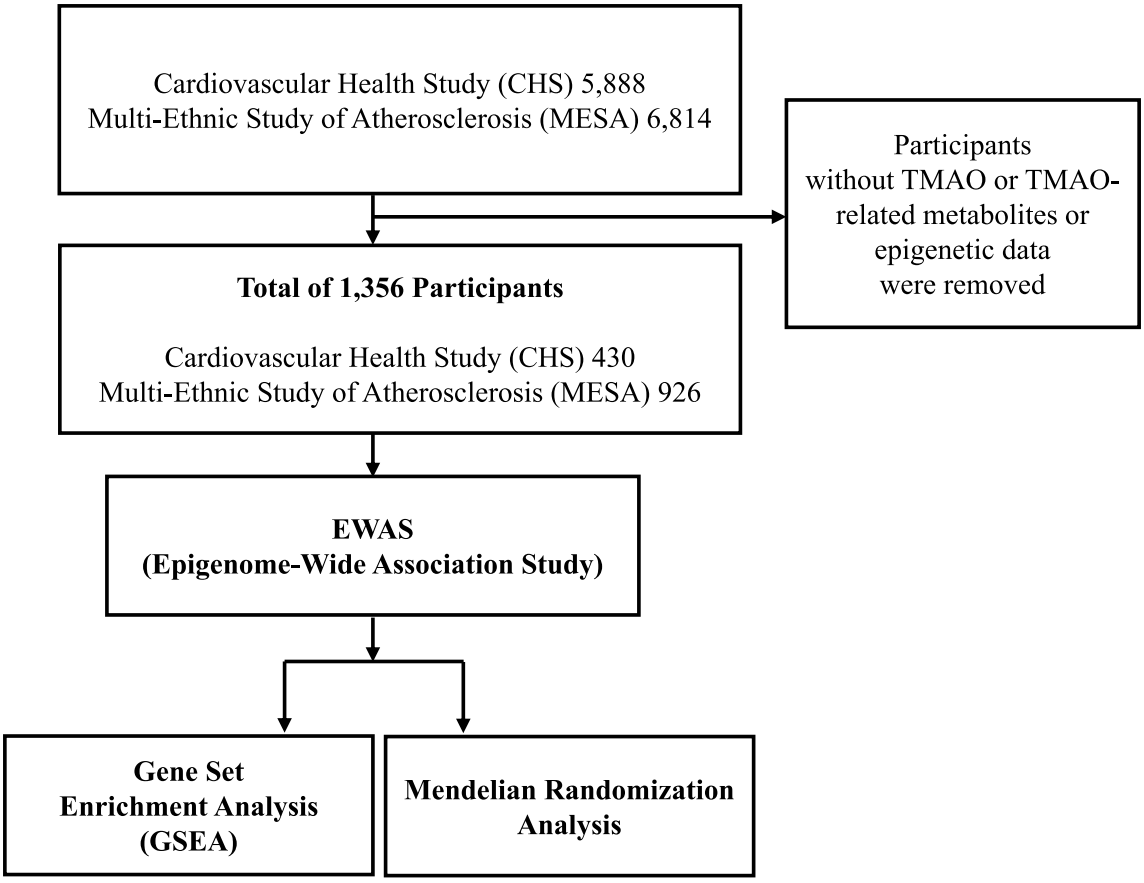

Fig. 1 Study design

random-effects meta-analysis to combine race/ethnicity-specific summary statistics within each cohort (i.e., race/ethnicity-specific analysis was performed in CHS and MESA separately). To aggregate results generated by the two cohorts, fixed-effects model meta-analysis was conducted. We defined CpGs with false discovery rate (FDR) < 0.05 statistically significant.

For CpGs that were significant in meta-analyses, we explored their potential biological functions based on information for genes related to these CpGs. Three sets of CpG-related genes were analyzed, including 1) annotated genes in the Illumina DNA methylation array supporting document, 2) *cis*-genes associated with these CpGs identified in the Framingham Heart Study [54], and 3) both *cis*- and *trans*-genes associated with these CpGs [54]. We defined *cis*-genes as nearby genes within 1 Mb from the CpG site with $P < 1e\text{-}7$ and *trans*-genes as remote genes residing > 1 Mb away from the CpG or at different chromosomes with $P < 1e\text{-}14$ [54]. We searched these genes in the Functional Mapping and Annotation of Genome-Wide Association Studies (FUMA) platform [55]. We also performed gene set enrichment analysis using the GSEA platform (version 4.3.3) based on the most updated Molecular Signature Database (MSigDB 2024.1.Hs) [56, 57]. Specifically, we analyzed MSigDB gene sets H, C2, C3-TFT, C5, C7, and C8. These gene sets have been integrated into the FUMA platform but were based on the earlier version of MSigDB (2023.1.Hs). Enrichment of CpG-related genes in gene sets was determined using the one-sided Fisher's exact test, and a test with Benjamini–Hochberg FDR < 0.05 was considered statistically significant.

To further explore whether metabolite-associated CpGs are associated with CVD, we used the *TwoSampleMR* R package [58] to test the putative causal association of these CpGs with CAD. DNA methylation quantitative loci (meQTL) SNPs identified by the Framingham Heart Study were analyzed [59]. We identified independent *cis*-meQTL SNPs after linkage disequilibrium (LD) pruning based on $R^2 < 0.01$ using the full 1000 Genome reference panel [60]. We extracted effect sizes and standard errors from the meQTL database [61], as well as from the summary results of a large GWAS for CAD [62]. We performed the primary analysis using the inverse variance weighted (IVW) method and sensitivity analysis using the MR-Egger method when we identified three or more independent SNPs. CpGs with FDR < 0.05 were considered significant.

Results

Participant characteristics

As shown in Table 1, 63% of CHS participants (n = 430) were women, compared to 53% in MESA (n = 926). In CHS, 53% of participants were European American (EA) and 47% were African American (AA). Whereas 42%, 29%, 20%, and 5% MESA participants were EA, AA, Hispanic American, and Chinese American, respectively. The CHS participants were on average 17 years older than those from MESA (mean age 77 vs. 60 years). Slightly fewer participants (9%) were current smokers in CHS than in MESA (14%). The amount of alcohol consumed and the overall dietary quality were modest in both cohorts. CHS participants had lower eGFR than those in MESA, 64.4 vs. 95.6 ml/min/1.73m^2.

EWAS of TMAO and TMAO-related metabolites

After adjusting for sex, age, study sites, blood cell composition, technical variables, education level, household income, and recent antibiotic use, our meta-analyses identified 4 CpGs associated with TMAO at FDR < 0.05 ($P \le 4.03e\text{-}7$; Table 2; Supplemental 1). Using the same model and at FDR < 0.05, we also identified 12, 53, 5, 6, and 63 CpGs for betaine ($P \le 1.19e\text{-}6$), γ-butyrobetaine ($P \le 6.11e\text{-}6$), carnitine ($P \le 5.42e\text{-}7$), choline ($P \le 2.81e\text{-}7$), and crotonobetaine ($P \le 7.25e\text{-}6$), respectively. Overall, 143 metabolite-CpG pairs were identified. Heterogeneity between the two cohorts was generally low to moderate for the majority of the 143 CpGs, 81 (57%) and 11 (8%) had $I^2 \le 25\%$ and 50%, respectively. Table 2 showed all CpGs with I^2 of 0. We found that no metabolites shared identical CpGs, and the pairwise correlation between these 143 CpGs was generally low (88% with Pearson $r < 0.3$ and 69% with Person $r < 0.1$). We presented 30 CpG pairs with $r \ge 0.5$ in Supplemental Table 2. For example, four TMAO-associated CpGs were moderately associated with four crotonobetaine-associated CpGs, r = 0.5. In addition, we found that many of the γ-butyrobetaine-associated CpGs were moderately associated with crotonobetaine-associated CpGs (Fig. 2). The highest r was -0.66 between cg04059696 (*MAPRE3*; γ-butyrobetaine, $P = 9.9e\text{-}7$) and cg17517296 (crotonobetaine, $P = 5.6e\text{-}6$). For most CpGs, further adjustment for sets 2 and 3 covariates (i.e., lifestyle factors, BMI, and eGFR) did not substantially alter the associations (Fig. 3; Supplemental Table 1).

Table 1 Participants' characteristics

	CHS	MESA
n	430	926
Age, years	77 ± 5	60 ± 10
Women, n (%)	272 (63%)	488 (53%)
BMI, kg/m2	27.7 ± 5.1	28.8 ± 5.2
Race/ethnicity (white; black, Hispanic; Chinese)	53%; 47%; 0%; 0%	42%; 20%; 30%; 8%
Smoking status (current; former; never)	9%; 46%; 45%	14%; 38%; 48%
Alcohol intake (drinks/week)	1.7 ± 6.0	2.7 ± 5.3
Physical activity	730 ± 1088	1711 ± 2656 (MET-min/week)
Dietary quality score	23.6 ± 5.2 (DASH)	40.9 ± 11.2 (AHEI)
Antibiotic use, n (%)	20 (5%)	22 (2%)
eGFR, mL/min/1.73m2	64.4 ± 19.1	95.6 ± 16.3

Gene set enrichment analysis

Using the 108 gene symbols annotated to all metabolite-associated CpGs by Illumina (Supplemental Table 3), we conducted enrichment analysis based on the most updated MSigDB gene sets. A total of 145 gene sets were significantly enriched (FDR < 0.05; Supplemental Table 3). Among 12 significant curated gene sets (CGS), three gene sets were particularly relevant to CVD risk: genes up-regulated in vascular smooth muscle cells by MAPK8 (CGS4; $P = 3.7e\text{-}6$) [63], genes down-regulated in the ventricles of the healthy hearts compared to atria (CGS5; $P = 4.5e\text{-}6$) [64], and down-regulated *cis*-regulated expression quantitative loci (*cis*-eQTL) in the heart that colocalized with previously mapped cardiac mass eQTLs (CGS8; $P = 4.7e\text{-}5$) [65]. Furthermore, 57 significant enrichments (FDR < 0.05) were observed in Human Phenotype Ontology gene sets (HPO) [66]. Six of those gene sets are associated with CVD, including abnormality of cardiovascular system electrophysiology (HPO6, $P = 1.8e\text{-}6$), abnormal heart morphology (HPO14, $P = 7.0e\text{-}6$; HPO19, $P = 1.8e\text{-}5$), vascular skin abnormality (HPO28, $P = 6.7e\text{-}5$), Abnormal myocardium morphology (HPO39, $P = 1.3e\text{-}4$), and thoracic aortic aneurysm (HPO55, $P = 2.5e\text{-}4$). In addition, there were 26 significant enrichments in Gene Ontology analysis (C5) and 17 in immunologic signatures (C7), 30 in Transcription Factors Targets (C3-TFT), and 4 Cell-type signatures (C8). Three TFT gene sets were enriched for genes containing one or more binding sites of DNMT1 ($P = 2.7e\text{-}5$), NKX2-5 ($P = 6.2e\text{-}4$), and KMT2D ($P = 9.7e\text{-}4$; Supplemental Table 3).

From the previously developed DNA methylation-associated gene expression database [54], we identified 74 *cis*-CpG-gene pairs (33 metabolite-associated CpGs and 70 genes) and 69 *trans*-CpG-gene pairs (5 metabolite-associated CpGs and 69 genes). When *cis*-genes were used in FUMA platform search, we found no significant enrichment at FDR < 0.05. However, the search using both *cis*- and *trans*-genes (132 genes with Ensembl ID) identified 198 enriched gene largest gene sets were from immunologic sets (Supplemental Table 4). The signatures (C7) [57]; the genes for metabolite-associated CpGs were enriched in 80 gene sets in this database. For example, the most enriched gene set in MsigDB C7 was

Table 2 Metabolite-CpG pairs with FDR < 0.05 and low heterogeneity in the fixed-effects meta

Metabolite	CpG	CHR	BP	Gene	CpG Island	Feature	Beta	SE	P	FDR
Betaine	cg01327202	1	17,215,511		Island	Enhancer, HMM Island, regulatory	-0.0088	0.0018	8.46e-07	0.037
Betaine	cg05712748	1	43,472,312		N_Shore	Enhancer,HMM Island	-0.0051	0.001	1.08e-07	0.007
Betaine	cg27032760	5	143,974,763		N_Shelf	HMM Island	-0.01	0.0019	1.09e-07	0.007
Betaine	cg18705301	15	41,695,430	NDUFAF1	S_Shore		-0.0263	0.0045	7.16e-09	0.001
Betaine	cg08914678	16	334,889	PDIA2	N_Shore	HMM Island, regulatory	0.0197	0.0026	1.34e-14	5.82e-09
Betaine	cg18593708	18	21,853,454	OSBPL1A	S_Shore		-0.0089	0.0018	5.55e-07	0.027
Butyrobetaine	cg24087235	1	54,665,621	CYB5RL;MRPL37	N_Shore	HMM Island, regulatory	0.0009	0.0002	3.96e-06	0.041
Butyrobetaine	cg17466510	1	116,877,566			Enhancer	0.0055	0.0012	3.24e-06	0.038
Butyrobetaine	cg20345923	2	1,983,190	MYT1L		HMM island	0.0052	0.001	1.51e-07	0.005
Butyrobetaine	cg04059696	2	27,211,953	MAPRE3		Enhancer	0.0051	0.001	9.89e-07	0.019
Butyrobetaine	cg05655116	2	37,899,435	CDC42EP3	Island	Enhancer, HMM Island, regulatory	0.0018	0.0004	2.79e-06	0.038
Butyrobetaine	cg03389926	2	42,651,266			Enhancer	0.0081	0.0017	1.55e-06	0.026
Butyrobetaine	cg03034070	2	190,044,841	COL5A2			-0.0119	0.0026	3.3e-06	0.038
Butyrobetaine	cg23339656	2	234,159,882	ATG16L1	N_Shore	Regulatory	0.0099	0.0018	4.35e-08	0.003
Butyrobetaine	cg16368147	4	62,111,221			Enhancer	0.0064	0.0014	3.36e-06	0.038
Butyrobetaine	cg05606878	5	126,432,189			Enhancer	0.0068	0.0015	4.86e-06	0.046
Butyrobetaine	cg02006915	5	175,991,129	PCDH24			0.0068	0.0015	4.49e-06	0.044
Butyrobetaine	cg26747317	6	31,829,793	NEU1	N_Shore		0.0093	0.0017	6.91e-08	0.004
Butyrobetaine	cg04346459	6	41,068,666	NFYA;LOC221442	Island	Enhancer, HMM island	0.0177	0.0033	7.36e-08	0.004
Butyrobetaine	cg09580153	6	41,068,724	NFYA;LOC221442	Island	Enhancer, HMM island	0.0101	0.0018	2.32e-08	0.003
Butyrobetaine	cg03644281	6	41,068,752	NFYA;LOC221442	Island	Enhancer, HMM island	0.0121	0.0023	1.11e-07	0.004
Butyrobetaine	cg07014126	6	169,717,713			HMM island	0.0042	0.0009	5.16e-06	0.046
Butyrobetaine	cg20109393	7	19,748,466	TWISTNB	Island	HMM Island, regulatory	-0.0004	0.0001	3.19e-06	0.038
Butyrobetaine	cg08500172	8	127,908,827			Enhancer	0.0043	0.0009	3.3e-06	0.038
Butyrobetaine	cg11009695	10	29,358,074			Enhancer	0.006	0.0013	6.11e-06	0.05
Butyrobetaine	cg00243281	11	2,597,838	KCNQ1	S_Shore	HMM_Island	0.004	0.0009	5.1e-06	0.046
Butyrobetaine	cg11527344	11	57,972,167	OR1S2			0.0037	0.0008	5.65e-06	0.048
Butyrobetaine	cg06079620	11	58,978,082	MPEG1			0.0058	0.0011	2.2e-07	0.006
Butyrobetaine	cg26561797	11	68,437,843		Island	HMM_Island	0.0048	0.0009	1.19e-07	0.004
Butyrobetaine	cg17306339	12	124,198,578	ATP6V0A2	S_Shore	DMR, regulatory	0.0072	0.0014	3.9e-07	0.01
Butyrobetaine	cg27481208	13	115,079,979	ZNF828	Island	Enhancer, HMM Island, regulatory	-0.0003	0.0001	3.32e-06	0.038
Butyrobetaine	cg23323891	14	57,200,519			Enhancer	0.0119	0.0026	3.54e-06	0.038
Butyrobetaine	cg18548879	15	41,914,454		S_Shore	HMM Island, Regulatory	0.0042	0.0009	1.24e-06	0.022
Butyrobetaine	cg10517312	15	45,027,253	TRIM69			0.0066	0.0012	1.34e-07	0.004
Butyrobetaine	cg01090433	16	82,673,506	CDH13		Enhancer, regulatory	0.0093	0.0019	1.06e-06	0.019
Butyrobetaine	cg10760240	17	35,414,006	AATF		HMM island	0.0077	0.0015	2.91e-07	0.008
Butyrobetaine	cg09309112	17	53,571,325			Enhancer	0.005	0.001	5.27e-07	0.012
Butyrobetaine	cg01885692	22	21,804,711	HIC2	S_Shelf	Enhancer	0.004	0.0009	5e-06	0.046
Carnitine	cg19408207	3	178,755,197	ZMAT3		Enhancer, regulatory	0.0078	0.0015	2.33e-07	0.034
Carnitine	cg06487937	16	5,116,160	C16orf89			-0.015	0.003	4.35e-07	0.047

Table 2 (continued)

Carnitine	cg21367586	18	34,327,498	FHOD3	S_Shore		0.0157	0.0022	2.19e-12	9.47e-07
Choline	cg15877769	4	1,062,280		N_Shore		0.0192	0.0037	2.81e-07	0.02
Choline	cg18875674	11	73,026,651	ARHGEF17		Enhancer	0.0101	0.0018	2.94e-08	0.003
Crotonobetaine	cg03396604	1	3,193,944	PRDM16	N_Shore		-0.0083	0.0018	7.1e-06	0.05
Crotonobetaine	cg13681752	1	120,143,242				0.005	0.0011	3.59e-06	0.035
Crotonobetaine	cg12730323	1	200,004,757	NR5A2	Island	DMR, Enhancer, HMM island	0.0042	0.0009	3.02e-06	0.035
Crotonobetaine	cg18794891	2	25,261,606		N_Shelf		0.0037	0.0008	7.21e-06	0.05
Crotonobetaine	cg08944893	2	105,461,870		S_Shore	Enhancer, DMR, HMM island	0.0028	0.0006	4.77e-06	0.04
Crotonobetaine	cg25975856	3	19,930,780	EFHB		Enhancer	0.0179	0.0039	5.6e-06	0.043
Crotonobetaine	cg24163658	3	58,182,370	DNASE1L3		Regulatory	0.0052	0.001	8.1e-07	0.025
Crotonobetaine	cg18073906	3	122,641,029	SEMA5B	Island	Enhancer, HMM island	0.0053	0.0011	1.86e-06	0.027
Crotonobetaine	cg17483361	4	54,243,829	FIP1L1	Island	Enhancer, HMM Island, regulatory	0.0011	0.0002	3.92e-08	0.005
Crotonobetaine	cg26298470	4	86,396,765	ARHGAP24		HMM island	0.0018	0.0004	7.08e-06	0.05
Crotonobetaine	cg13900348	5	76,114,646	F2RL1	Island	HMM Island, regulatory	0.0018	0.0004	3.84e-06	0.036
Crotonobetaine	cg10812634	5	126,409,211	FLJ44606	Island	HMM Island, Regulatory	0.0124	0.0026	1.75e-06	0.027
Crotonobetaine	cg27183454	6	28,547,741	SCAND3			0.0038	0.0008	5.4e-06	0.042
Crotonobetaine	cg02718200	6	31,324,269	HLA-B	Island	HMM Island, regulatory,	0.0057	0.0012	1.4e-06	0.027
Crotonobetaine	cg18419694	6	143,832,440	FUCA2	Island	Enhancer, HMM Island, regulatory	-0.0009	0.0002	5.13e-06	0.041
Crotonobetaine	cg10146442	7	884,056	UNC 84A;UNC 84A	N_Shelf	HMM island	-0.0059	0.0006	1.93e-25	8.33e-20
Crotonobetaine	cg18669823	7	30,725,669		S_Shelf		-0.009	0.0017	6.1e-08	0.005
Crotonobetaine	cg14299044	10	19,972,179			Enhancer	0.0025	0.0006	4.21e-06	0.037
Crotonobetaine	cg02979795	10	102,626,509			Enhancer, HMM Island, regulatory	0.0093	0.0019	1.68e-06	0.027
Crotonobetaine	cg03900474	12	115,106,786		S_Shore	Enhancer	0.0025	0.0006	7.25e-06	0.05
Crotonobetaine	cg20005934	14	100,706,390	YY1	Island	Enhancer, HMM Island, regulatory	-0.0006	0.0001	2.68e-06	0.032
Crotonobetaine	cg03469805	14	105,330,648	KIAA0284	Island	HMM island	0.0049	0.001	1.53e-06	0.027
Crotonobetaine	cg03643241	15	44,487,910	FRMD5	S_Shore	Regulatory	0.0042	0.0009	1.39e-06	0.027
Crotonobetaine	cg01283685	16	2,986,893	FLYWCH1			-0.01	0.0021	2.58e-06	0.032
Crotonobetaine	cg20215112	17	43,065,055			Enhancer, regulatory	0.0039	0.0008	1.43e-06	0.027
Crotonobetaine	cg01737415	17	72,919,525	OTOP2;USH1G	Island	Enhancer, HMM island, regulatory	0.0035	0.0007	1.21e-06	0.027
Crotonobetaine	cg14884776	19	15,122,181	CCDC105	S_Shore		0.0033	0.0007	2.08e-06	0.028

Table 2 (continued)

TMAO	cg20768669	1	149,137,508		N_Shore	Regulatory	0.0075	0.0015	3.59e-07	0.044
TMAO	cg07152869	16	27,741,555	KIAA0556		Enhancer	-0.0125	0.0023	1.06e-07	0.039

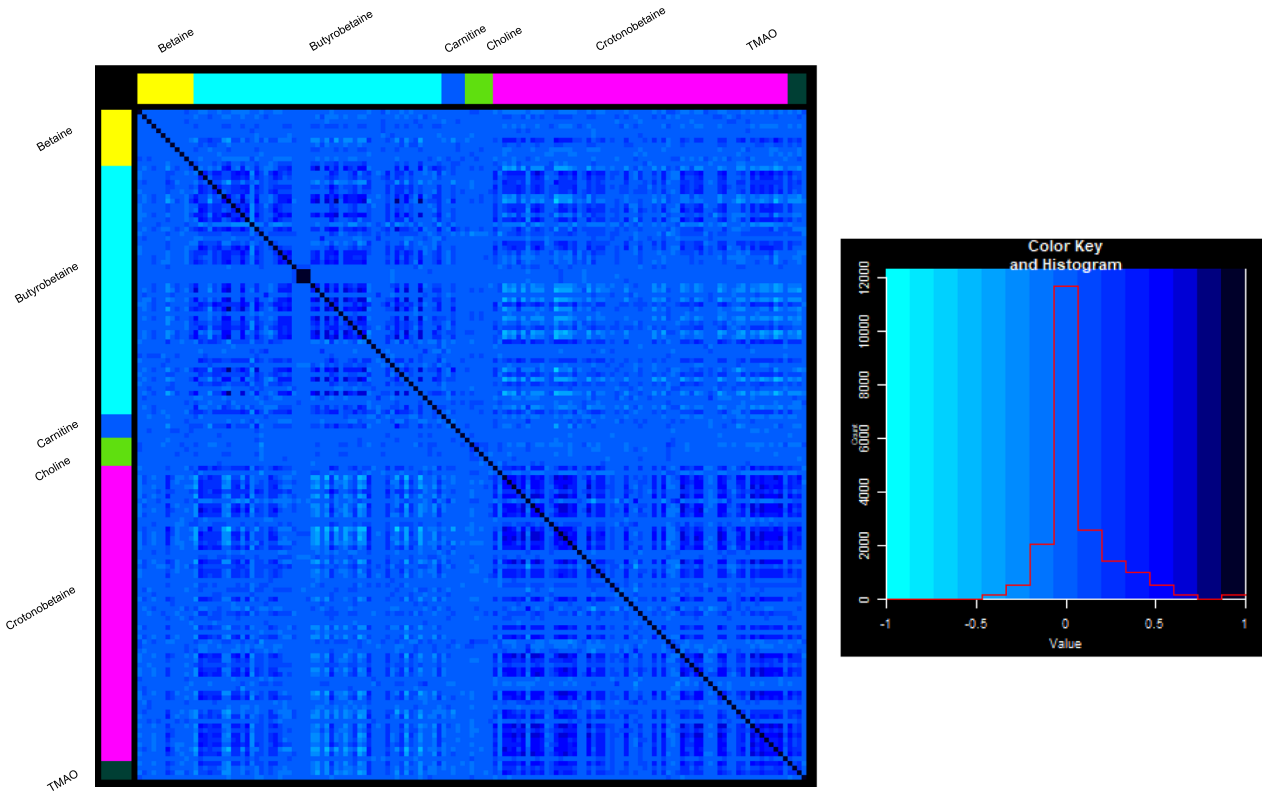

Fig. 2 Pairwise Pearson correlation between the 143 CpGs associated with TMAO and TMAO-related metabolites. Squares in heatmap and the sidebars are for metabolite-specific metabolites. The heatmap was generated using MESA DNA methylation data

GSE4984 for immunologic signatures (genes down-regulated in monocyte-derived dendritic cells control versus treated with LGALS1) [67], $P = 6.4e\text{-}32$. The enriched genes in this gene set included 25 *trans*-genes associated with cg06079620 (*MPEG1*), a CpG associated with γ-butyrobetaine ($P = 2.2e\text{-}7$). In addition, 77 CpG-associated genes were enriched in these 198 gene sets. In these 77 genes, 37 (48%) were *trans*-genes for cg06079620. Like we observed in analyses using Illumina annotated genes, results from searching the most updated GESA platform yielded more enriched gene sets (n = 289) at FDR < 0.05 (Supplemental Table 5); however, the overall pattern was similar to the FUMA platform search, e.g., the largest gene sets were from immunologic signatures (C7; n = 100 gene sets).

MR analysis

We extracted *cis*-meQTL SNPs for 101 CpGs. MR analyses were successfully performed for 90 CpGs for CAD. At FDR < 0.05, we found three CpGs were putatively causal to CAD (Table 3). CpG cg18705301 (*NDUFAF1*) was inversely associated with betaine concentrations ($P = 7.2e\text{-}9$). The MR analysis showed hypermethylation at this CpG (cg18705301) was associated with a lower risk of CAD ($P = 1.8e\text{-}5$). We also found that cg06073535, a CpG positively associated with γ-butyrobetaine ($P = 3.6e\text{-}8$), was inversely associated with CAD risk in MR analysis ($P = 3.2e\text{-}4$). Cg10146442 (*SUN1*) was inversely associated with crotonobetaine concentrations ($P = 1.8e\text{-}6$), and higher levels of DNA methylation at this CpG were associated with an increased CAD risk ($P = 7.4e\text{-}4$). MR Egger analysis also showed a similar association at cg10146442 ($P = 0.004$; Fig. 4). For all three CpGs, we found no significant heterogeneity and horizontal pleiotropy (Table 3).

Discussion

In this study examining a diverse sample of U.S. adults, we identified several DNA methylation markers associated with quantitative measures of circulating TMAO and TMAO-related metabolites. Most identified CpGs (116 of 143) were associated with two TMAO precursors: γ-butyrobetaine and crotonobetaine. Using annotated genes for these CpGs, gene set enrichment analysis identified three corresponding curated gene sets (including

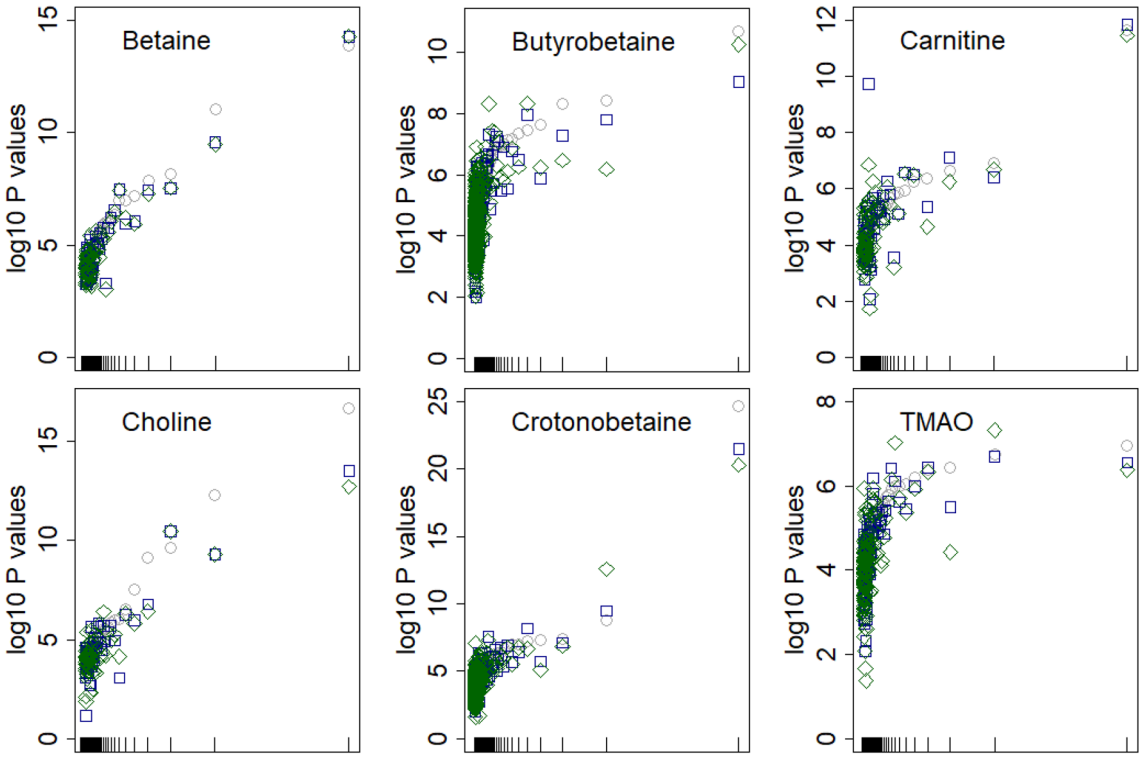

Fig. 3 Meta-analysis P values from models adjusting for three sets of covariates. Grey circles were from models with adjustment for sex, age, race/ethnicity, study sites, blood cells composition, technical variables, education level, household income, and recent antibiotic use. CpGs with P < 1e-4 in this model were included. Blue squares were from models with additional adjustment for smoking status, alcohol intake, physical activity, and diet quality scores. Green diamonds were from models with additional adjustment for BMI and eGFR. Y axis is the -log10 P values and X axis represents CpGs ordered by P value significance from low (left) to high (right). Each bar at x-axis represents one CpG

Table 3 MR analysis for TMAO and TMAO-related metabolites and CAD ME Egger

						Heteroge	**intercept**	**Number**	**MR**	**CpG-associated**
CpG	Gene	Beta	SE	P	FDR	neity P	P	of SNPs	Egger P	Metabolites
cg18705301	NDUFAF1	-0.23	0.05	1.8E-05	0.002	0.54	0.96	16	0.12	Betaine
cg06073535		-1.99	0.55	3.2E-04	0.015	0.55	0.57	15	0.05	Butyrobetaine
cg10146442	SUN1	0.15	0.05	7.4E-04	0.022	0.21	0.17	21	0.004	Crotonobetaine

canonical pathways) and six human disease gene sets (human phenotype ontology) that have broad biological impacts on cardiovascular health. Further analysis using associated genes identified more enriched gene sets such as those from immunologic signatures. Our MR analysis using published GWAS databases also suggests that γ-butyrobetaine- and crotonobetaine-associated CpGs may affect CVD risk. Taken together, the present study suggests that epigenetic regulations are involved in the pathways linking TMAO and TMAO-related metabolites and CVD risk.

TMAO production is dependent on the oxidation of dietary substates, including choline and *L*-carnitine, by the gut microbes [68]. During this process, dietary *L*-carnitine is converted to γ-butyrobetaine and crotonobetaine, important precursors of TMAO; further, some evidence suggests γ-butyrobetaine and crotonobetaine can be converted to each other [2]. Previous studies have suggested that both γ-butyrobetaine and crotonobetaine may have their own potential pathogenic effects on cardiometabolic diseases [1, 2]. In the present study, we demonstrated that both γ-butyrobetaine and crotonobetaine were associated with DNA methylation status at a large number of CpG sites across several chromosomes. In line with the biological connection between TMAO, γ-butyrobetaine, and crotonobetaine, we found several CpGs associated with these three metabolites were moderately correlated (i.e., CpG pairs in Supplemental Table2). Interestingly, these CpGs generally reside in different chromosomes, suggesting that TMAO and related metabolites are related to both *cis*- and *trans*-methylation regulations.

Our gene enrichment analysis with genes where CpG were associated with TMAO and TMAO-related metabolites identified gene sets with dysregulated expressions correlated with abnormality of cardiovascular physiology

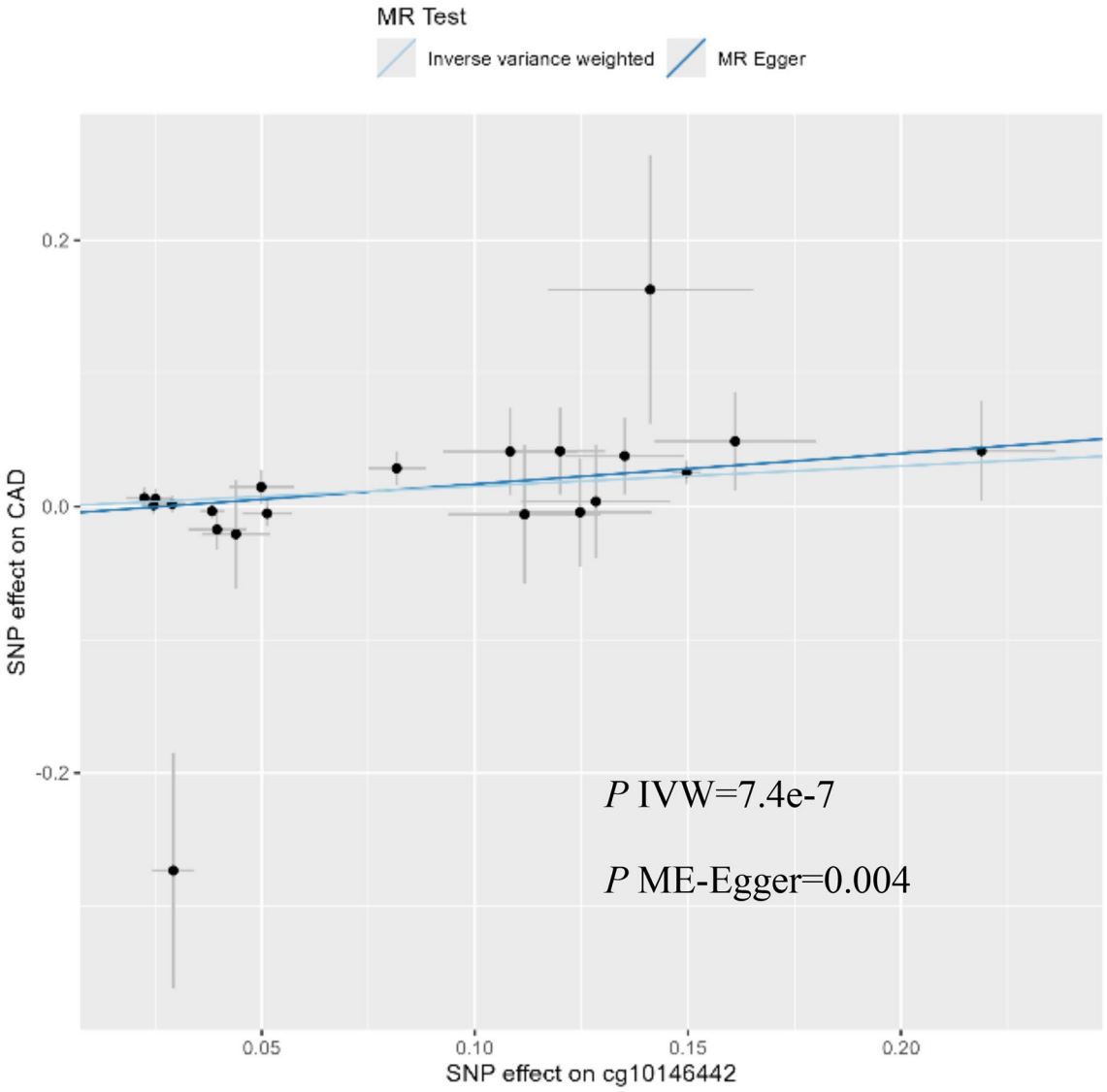

Fig. 4 MR analysis for cg10146442 and CAD

or morphology [63, 66]. Among gene sets highly relevant to CVD, six shared the gene *NDUFAF1* (ubiquinone oxidoreductase complex assembly factor 1). Missense mutations in the *NDUFAF1* gene cause infantile hypertrophic cardiomyopathy [69]. In addition, abnormal expression of the *NDUFAF1* gene can also lead to mitochondrial oxidative phosphorylation dysfunction, thereby causing CVD [70]. Complementing the evidence, our MR analysis further indicated that DNA methylation of *NDUFAF1* may be involved in the pathogenic process associated with the two TMAO precursors.

MR analysis also identified another CpG site at the *SUN1* gene that may be causally involved in CVD [71]. Of the 30 transcription factor target (TFT) gene sets identified by gene enrichment analysis, three TFT gene sets shared *SUN1*, which contains one or more *DNMT1*, *NKX2-5*, and *KMT2D* binding sites. *DNMT1* is a DNA methyltransferase I and *KMT2D* is a histone methyltransferase, which may broadly affect CVD risk. *NKX2-5* is a transcription factor that plays a role in heart formation and development, and population studies have shown that genetic variation in *NKX2-5* was associated with congenital heart disease [72]. Our MR analysis identified three CpGs (cg18705301, cg06073535, and cg10146442) potentially causal to CAD. We conducted this analysis using a single meQTL database derived from the Framingham Heart Study [59]. We searched the meQTLs for the three significant CpGs in the Genetics of DNA Methylation Consortium (GoDMC) database http://mqtldb.godmc.org.uk), but did not find any SNPs for these three CpGs. Therefore, our observations may be biased and future studies utilizing independent meQTL databases

are needed to verify our findings. In the Illumina DNA methylation annotation document, the genes *NDUFAF1* and *SUN1* were assigned to cg18705301 and cg10146442, respectively. In a previously published database of CpG-gene transcript pairs [54], we found that the three CpGs were also associated with other *cis*-genes, e.g., cg10146442 associated with three nearby genes *SUN1*, *DNAAF5*, and *GET4*. Therefore, the biological pathways linking these CpGs to CAD need future exploration.

A previous study in 847 participants from the Genetics of Lipid Lowering Drugs and Diet Network (GOLDN) found no significant association between TMAO levels and DNA methylation after correcting for epigenome-wide tests ($P < 1.1e\text{-}7$) [29]. We searched the top 10 CpGs in the GOLDN study and found none with $P < 0.05$ in our summary statistics. The discrepancy may be due to the different approach for TMAO measurement, which in the GOLDN study was performed by proton nuclear magnetic resonance (NMR) spectroscopy [29], compared to our approach using a stable-isotope dilution assay coupled with high-performance liquid chromatography. In addition, the GOLDN study measured DNA methylation from CD4 + T-cells, whereas we used whole blood DNA samples, suggesting tissue-specificity may affect TMAO-related DNA methylation status. Notably, the GOLDN study did not simultaneously evaluate the other TMAO-related metabolites [29], many of which showed multiple DNA methylation signatures. Our new results suggest the need for further analyses to understand factors that may affect the relationship between TMAO, its related metabolites, and DNA methylation in different cells and tissues.

Betaine is an essential methyl donor [74] and plays an important role in DNA methylation [75]. The Melbourne Collaborative Cohort Study found no significant associations between estimated dietary betaine intake (based on a self-reported food frequency questionnaire) and DNA methylation among 5,186 adults [76]. In addition, the correlation between estimated dietary betaine and plasma betaine was low (age- and sex-adjusted $r \sim 0.1$) [77], which could relate to errors in estimates of self-reported betaine intake, or low responsiveness of plasma betaine to dietary intake [78]. Reasons for the difference between the previous study [76] and ours are unclear. The finding in our MR analysis was consistent with a previous study demonstrating a positive association of higher plasma betaine levels with increased CVD risk [79]. Nonetheless, future studies with large sample sizes and diverse background are warranted to validate our findings and to explore potential mechanisms.

Our study has several strengths. First, we used a robust approach to measure TMAO and TMAO-related metabolites. TMAO and TMAO-metabolites are commonly included in broad metabolomic panels. However, these methods reduce measurement accuracy compared with calibrated measurements using isotope labeled internal standards and methodology optimized for quantitative results, as is used in the present study. CHS and MESA have used both measurement approaches to quantify plasma metabolites; thus, data from these cohorts will provide valuable insights for future analysis. Second, we included a diverse sample from two well-established community-based cohorts. Both cohorts have collected and validated a comprehensive list of data (e.g., lifestyle, biomarkers, and clinical factors), which allowed us to carefully consider potential impacts of these factors in metabolite-CpG association analysis. For most metabolite-CpG pairs, the association remained stable with additional adjustment for these factors.

Some limitations are noticed in this study. We cannot exclude residual confounding due to measurement errors or unmeasured factors. A bidirectional MR analysis may provide a potential causal relationship between metabolites and CpGs. However, large genetic association analysis is currently lacking for metabolites measured using the same approach we used. Future studies are needed to clarify the causal relationships between metabolites and DNA methylation. Other limitations should also be considered. We found loci in which multiple CpGs showed concordant significance, whereas, in several loci, a single CpG was statistically significant. Such results may represent a technically false positive and validation in independent study samples is needed. Although we meta-analyzed cohort-specific results from CHS and MESA, including additional samples and external validation cohorts will strengthen our analysis. We highlighted a few enriched gene sets such as those from immunologic signatures. We conducted these enrichment analyses using either annotated or associated genes, which may not reflect the genes affected by metabolite-associated CpGs in our specific study participants. Therefore, these findings should be interpreted with caution.

In conclusion, we identified DNA methylation loci that were associated with TMAO and its related metabolites in a group of middle-aged to older adults. Our bioinformatic analyses further suggest these DNA methylation loci may affect cardiovascular health via multiple pathways. Future studies with large sample sizes and diverse populations are needed to validate our observations and investigate the clinical impacts of these DNA methylation loci.

Supplementary Information

The online version contains supplementary material available at https://doi.org/10.1186/s13148-026-02060-w.

Additional file1 (DOCX 25 KB)

Additional file2 (PDF 777 KB)

Acknowledgements
The authors thank the other investigators, the staff, and the participants of the MESA study for their valuable contributions. A full list of participating MESA investigators and institutes can be found at http://www.mesa-nhlbi.org. A full list of principal CHS investigators and institutions can be found at CHS-NHLBI.org. We gratefully acknowledge the studies and participants who provided biological samples and data for TOPMed.

Disclaimer
The content is solely the responsibility of the authors and does not necessarily represent the official views of the National Institutes of Health.

Disclosure
Z.W. and S.L.H. report being named as co-inventor on pending and issued patents held by the Cleveland Clinic relating to cardiovascular diagnostics and therapeutics. S.L.H. also reports being a paid consultant for Zehna Therapeutics. S.L.H. reports having received research funds from Procter & Gamble, Zehna Therapeutics and Roche Diagnostics. Z.W. and S.L.H. report being eligible to receive royalty payments for inventions or discoveries related to cardiovascular diagnostics or therapeutics from Cleveland Heart Lab, and Procter & Gamble, and S.L.H. from Zehna Therapeutics. B.M.P. serves on the Steering Committee of the Yale Open Data Access Project funded by Johnson & Johnson.

Author contributions
Jiantao Ma, Chao-Qiang Lai, and Dariush Mozaffarian were responsible for the study design. Jiantao Ma, Chao-Qiang Lai, Xiuqing Guo, Jennifer A. Brody, and Soyoung Lee conducted the data analysis. Jiantao Ma, Chao-Qiang Lai, Dariush Mozaffarian, and Soyoung Lee were responsible for manuscript writing. Stanley L. Hazen and Dariush Mozaffarian provided funding support. Soyoung Lee and Meng Wang were responsible for data management. All other authors including Xinmin S Li, Zeneng Wang, Jie Yao, Kent D. Taylor, Russell P. Tracy, Durda Peter, Yongmei Liu, Jerome I. Rotter, Stephen S. Rich, Matthew Budoff, W H Wilson Tang, Joseph A DiDonato, Rozenn N. Lemaitre, Nona Sotoodehnia, Bruce M. Psaty, José M. Ordovás, and David S. Siscovick contributed to critical review of the study proposal and manuscript.

Funding
The MESA projects are conducted and supported by the National Heart, Lung, and Blood Institute (NHLBI) in collaboration with MESA investigators. Support for the Multi-Ethnic Study of Atherosclerosis (MESA) projects are conducted and supported by the National Heart, Lung, and Blood Institute (NHLBI) in collaboration with MESA investigators. Support for MESA is provided by contracts 75N92020D00001, HHSN268201500003I, N01-HC-95159, 75N92020D00005, N01-HC-95160, 75N92020D00002, N01-HC-95161, 75N92020D00003, N01-HC-95162, 75N92020D00006, N01-HC-95163, 75N92020D00004, N01-HC-95164, 75N92020D00007, N01-HC-95165, N01-HC-95166, N01-HC-95167, N01-HC-95168, N01-HC-95169, UL1-TR-000040, UL1-TR-001079, UL1-TR-001420, UL1TR001881, DK063491, and R01HL105756. The CHS research was supported by NHLBI contracts HHSN268201200036C, HHSN268200800007C, HHSN268201800001C, N01HC55222, N01HC85079, N01HC85080, N01HC85081, N01HC85082, N01HC85083, N01HC85086, 75N92021D00006; and NHLBI grants U01HL080295, U01HL130114, K08HL116640, R01HL087652, R01HL092111, R01HL103612, R01HL105756, R01HL111089, R01HL116747, R01HL120393 and R01HL172803 with additional contribution from the National Institute of Neurological Disorders and Stroke (NINDS). Additional support was provided through R01AG023629 from the National Institute on Aging (NIA), Merck Foundation / Society for Epidemiologic Research as well as Laughlin Family, Alpha Phi Foundation, and Locke Charitable Foundation. The provision of genotyping data was supported in part by the National Center for Advancing Translational Sciences, CTSI grant UL1TR000124, and the National Institute of Diabetes and Digestive and Kidney Disease Diabetes Research Center (DRC) grant DK063491 to the Southern California Diabetes Endocrinology Research Center. MESA and CHS were partly supported by the Trans-Omics in Precision Medicine (TOPMed) program, the National Heart, Lung and Blood Institute (NHLBI). Molecular data for the TOPMed program was supported by the NHLBI. Methylomics for "NHLBI TOPMed: MESA (phs001416) was performed at Keck Molecular Genomics Core Facility (HHSN268201600034I). Core support including centralized genomic read mapping and genotype calling, along with variant quality metrics and filtering were provided by the TOPMed Informatics Research Center (3R01HL-117626-02S1; contract HHSN268201800002I). Core support including phenotype harmonization, data management, sample-identity QC, and general program coordination were provided by the TOPMed Data Coordinating Center (R01HL-120393; U01HL-120393; contract HHSN268201800001I). These studies were supported by NIH grant R01 HL135920-5. SLH was also supported by NIH grants P01HL147823 and R01HL103866.

Data availability
The data described in the manuscript are available at dbGap (Accession ID for CHS: phs000287.v7.p1 and Accession ID for MESA: phs000209.v13.p3) upon research proposal approval from dbGap.

Declarations

Ethics approval
The study was approved by the Tufts Institutional Review Board. All participants provided written informed consent, and all research was conducted in accordance with the Declaration of Helsinki.

Consent to publish
All authors consent to publish declarations.

Competing interests
Conflict of interest Z.W. and S.L.H. report being named as co-inventor on pending and issued patents held by the Cleveland Clinic relating to cardiovascular diagnostics and therapeutics. S.L.H. also reports being a paid consultant for Zehna Therapeutics. S.L.H. reports having received research funds from Procter & Gamble, Zehna Therapeutics and Roche Diagnostics. Z.W. and S.L.H. report being eligible to receive royalty payments for inventions or discoveries related to cardiovascular diagnostics or therapeutics from Cleveland Heart Lab, and Procter & Gamble, and S.L.H. from Zehna Therapeutics. B.M.P. serves on the Steering Committee of the Yale Open Data Access Project funded by Johnson & Johnson.

Author details
[1]Friedman School of Nutrition Science and Policy, Tufts University, Boston, MA, USA
[2]USDA ARS, Jean Mayer USDA Human Nutrition Research Center On Aging, Boston, MA, USA
[3]Department of Heart, Blood and Kidney Research, Learner Research Institute, Cleveland Clinic, Cleveland, OH, USA
[4]Department of Pediatrics, The Institute for Translational Genomics and Population Sciences, Lundquist Institute for Biomedical Innovation at Harbor-UCLA Medical Center, Torrance, CA, USA
[5]Department of Pathology & Laboratory Medicine, University of Vermont Larner College of Medicine, 360 South Park Drive, Colchester, VT 05446, USA
[6]Duke Molecular Physiology Institute, Duke University, Durham, NC, USA
[7]Department of Genome Sciences, University of Virginia School of Medicine, 1200 Jefferson Park Avenue, Charlottesville, VA 22903, USA
[8]Department of Medicine, Lundquist Institute at Harbor-UCLA Medical Center, Torrance, CA, USA
[9]Department of Cardiovascular Medicine, Cleveland Clinic, Heart, Vascular and Thoracic Institute, Cleveland, OH, USA
[10]Cardiovascular Health Research Unit, Department of Medicine, University of Washington, Seattle, WA, USA
[11]Cardiovascular Health Research Unit, Departments of Medicine, Epidemiology, and Health Systems and Population Health, University of Washington, Seattle, WA, USA
[12]Jean Mayer USDA Human Nutrition Research Center On Aging, Boston, MA, USA
[13]New York Academy of Medicine, New York, NY, USA

Received: 30 September 2025 / Accepted: 13 January 2026
Published online: 09 February 2026

References

1. Wang M, Wang Z, Lee Y, Lai HTM, de Oliveira Otto MC, Lemaitre RN, et al. Dietary Meat, Trimethylamine N-Oxide-Related Metabolites, and Incident

Cardiovascular Disease Among Older Adults: The Cardiovascular Health Study. Arterioscler Thromb Vasc Biol. 2022;42(9):e273–88.
2. Koeth RA, Levison BS, Culley MK, Buffa JA, Wang Z, Gregory JC, et al. gamma-Butyrobetaine is a proatherogenic intermediate in gut microbial metabolism of L-carnitine to TMAO. Cell Metab. 2014;20(5):799–812.
3. Wang Z, Klipfell E, Bennett BJ, Koeth R, Levison BS, Dugar B, et al. Gut flora metabolism of phosphatidylcholine promotes cardiovascular disease. Nature. 2011;472(7341):57–63.
4. Roberts AB, Gu X, Buffa JA, Hurd AG, Wang Z, Zhu W, et al. Development of a gut microbe-targeted nonlethal therapeutic to inhibit thrombosis potential. Nat Med. 2018;24(9):1407–17.
5. Buffa JA, Romano KA, Copeland MF, Cody DB, Zhu W, Galvez R, et al. The microbial gbu gene cluster links cardiovascular disease risk associated with red meat consumption to microbiota L-carnitine catabolism. Nat Microbiol. 2022;7(1):73–86.
6. Wang Z, Roberts AB, Buffa JA, Levison BS, Zhu W, Org E, et al. Non-lethal Inhibition of Gut Microbial Trimethylamine Production for the Treatment of Atherosclerosis. Cell. 2015;163(7):1585–95.
7. Tang WH, Wang Z, Kennedy DJ, Wu Y, Buffa JA, Agatisa-Boyle B, et al. Gut microbiota-dependent trimethylamine N-oxide (TMAO) pathway contributes to both development of renal insufficiency and mortality risk in chronic kidney disease. Circ Res. 2015;116(3):448–55.
8. Benson TW, Conrad KA, Li XS, Wang Z, Helsley RN, Schugar RC, et al. Gut Microbiota-Derived Trimethylamine N-Oxide Contributes to Abdominal Aortic Aneurysm Through Inflammatory and Apoptotic Mechanisms. Circulation. 2023;147(14):1079–96.
9. Organ CL, Li Z, Sharp TE 3rd, Polhemus DJ, Gupta N, Goodchild TT, et al. Nonlethal inhibition of gut microbial trimethylamine N-oxide production improves cardiac function and remodeling in a murine model of heart failure. J Am Heart Assoc. 2020;9(10):e016223.
10. Gupta N, Buffa JA, Roberts AB, Sangwan N, Skye SM, Li L, et al. Targeted inhibition of gut microbial trimethylamine N-oxide production reduces renal tubulointerstitial fibrosis and functional impairment in a murine model of chronic kidney disease. Arterioscler Thromb Vasc Biol. 2020;40(5):1239–55.
11. Warrier M, Shih DM, Burrows AC, Ferguson D, Gromovsky AD, Brown AL, et al. The TMAO-Generating Enzyme Flavin Monooxygenase 3 Is a Central Regulator of Cholesterol Balance. Cell Rep. 2015;10(3):326–38.
12. Ge P, Duan H, Tao C, Niu S, Hu Y, Duan R, et al. TMAO Promotes NLRP3 Inflammasome Activation of Microglia Aggravating Neurological Injury in Ischemic Stroke Through FTO/IGF2BP2. J Inflamm Res. 2023;16:3699–714.
13. Canyelles M, Borras C, Rotllan N, Tondo M, Escola-Gil JC, Blanco-Vaca F. Gut microbiota-derived TMAO: a causal factor promoting atherosclerotic cardiovascular disease? Int J Mol Sci. 2023. https://doi.org/10.3390/ijms24031940.
14. Seldin MM, Meng Y, Qi H, Zhu W, Wang Z, Hazen SL, et al. Trimethylamine N-oxide promotes vascular inflammation through signaling of mitogen-activated protein kinase and nuclear factor-κB. J Am Heart Assoc. 2016;5(2):e002767.
15. Shanmugham M, Devasia AG, Chin YL, Cheong KH, Ong ES, Bellanger S, et al. Time-dependent specific molecular signatures of inflammation and remodelling are associated with trimethylamine-N-oxide (TMAO)-induced endothelial cell dysfunction. Sci Rep. 2023;13(1):20303.
16. Skye SM, Zhu W, Romano KA, Guo CJ, Wang Z, Jia X, et al. Microbial transplantation with human gut commensals containing CutC is sufficient to transmit enhanced platelet reactivity and thrombosis potential. Circ Res. 2018;123(10):1164–76.
17. Emonds JJ, Ringel C, Reinicke M, Muller D, Von Eckardstein A, Meixensberger J, et al. Influence of trimethylamine N-oxide on platelet activation. Nutrients. 2022. https://doi.org/10.3390/nu14163261.
18. Zhu W, Gregory JC, Org E, Buffa JA, Gupta N, Wang Z, et al. Gut microbial metabolite TMAO enhances platelet hyperreactivity and thrombosis risk. Cell. 2016;165(1):111–24.
19. Ma J, Rebholz CM, Braun KVE, Reynolds LM, Aslibekyan S, Xia R, et al. Whole Blood DNA Methylation Signatures of Diet Are Associated With Cardiovascular Disease Risk Factors and All-Cause Mortality. Circ Genom Precis Med. 2020;13(4):e002766.
20. Joehanes R, Just AC, Marioni RE, Pilling LC, Reynolds LM, Mandaviya PR, et al. Epigenetic Signatures of Cigarette Smoking. Circ Cardiovasc Genet. 2016;9(5):436–47.
21. Mendelson MM, Marioni RE, Joehanes R, Liu C, Hedman AK, Aslibekyan S, et al. Association of body mass index with DNA methylation and gene expression in blood cells and relations to cardiometabolic disease: a mendelian randomization approach. PLoS Med. 2017;14(1):e1002215.
22. Richard MA, Huan T, Ligthart S, Gondalia R, Jhun MA, Brody JA, et al. DNA Methylation Analysis Identifies Loci for Blood Pressure Regulation. Am J Hum Genet. 2017;101(6):888–902.
23. Zheng Y, Joyce BT, Hwang SJ, Ma J, Liu L, Allen NB, et al. Association of cardiovascular health through young adulthood with genome-wide DNA methylation patterns in midlife: the CARDIA study. Circulation. 2022;146(2):94–109.
24. Agha G, Mendelson MM, Ward-Caviness CK, Joehanes R, Huan T, Gondalia R, et al. Blood leukocyte DNA methylation predicts risk of future myocardial infarction and coronary heart disease. Circulation. 2019;140(8):645–57.
25. Battram T, Yousefi P, Crawford G, Prince C, Sheikhali Babaei M, Sharp G, et al. The EWAS catalog: a database of epigenome-wide association studies. Wellcome Open Res. 2022;7:41.
26. Romano KA, Martinez-del Campo A, Kasahara K, Chittim CL, Vivas EI, Amador-Noguez D, et al. Metabolic, Epigenetic, and Transgenerational Effects of Gut Bacterial Choline Consumption. Cell Host Microbe. 2017;22(3):279–90.
27. Obeid R, Awwad HM, Rabagny Y, Graeber S, Herrmann W, Geisel J. Plasma trimethylamine N-oxide concentration is associated with choline, phospholipids, and methyl metabolism. Am J Clin Nutr. 2016;103(3):703–11.
28. Friso S, Udali S, De Santis D, Choi SW. One-carbon metabolism and epigenetics. Mol Aspects Med. 2017;54:28–36.
29. Aslibekyan S, Irvin MR, Hidalgo BA, Perry RT, Jeyarajah EJ, Garcia E, et al. Genome- and CD4+ T-cell methylome-wide association study of circulating trimethylamine-N-oxide in the Genetics of Lipid Lowering Drugs and Diet Network (GOLDN). Journal of Nutrition & Intermediary Metabolism. 2017;8:1–7.
30. Bild DE, Bluemke DA, Burke GL, Detrano R, Diez Roux AV, Folsom AR, et al. Multi-Ethnic Study of Atherosclerosis: objectives and design. Am J Epidemiol. 2002;156(9):871–81.
31. Fried LP, Borhani NO, Enright P, Furberg CD, Gardin JM, Kronmal RA, et al. The cardiovascular health study: design and rationale. Ann Epidemiol. 1991;1(3):263–76.
32. Wang Z, Levison BS, Hazen JE, Donahue L, Li XM, Hazen SL. Measurement of trimethylamine-N-oxide by stable isotope dilution liquid chromatography tandem mass spectrometry. Anal Biochem. 2014;455:35–40.
33. Wang Z, Bergeron N, Levison BS, Li XS, Chiu S, Jia X, et al. Impact of chronic dietary red meat, white meat, or non-meat protein on trimethylamine N-oxide metabolism and renal excretion in healthy men and women. Eur Heart J. 2019;40(7):583–94.
34. Hu X, Logan JG, Kwon Y, Lima JAC, Jacobs DR, Duprez D, et al. Multi-ancestry epigenome-wide analyses identify methylated sites associated with aortic augmentation index in TOPMed MESA. Sci Rep. 2023;13(1):17680.
35. Levy D, Kirmani S, Huan T, Van Amburg J, Joehanes R, Uddin MM, et al. Epigenome-wide DNA Methylation Association Study of CHIP Provides Insight into Perturbed Gene Regulation. Res Sq. 2024.
36. Pidsley R, Zotenko E, Peters TJ, Lawrence MG, Risbridger GP, Molloy P, et al. Critical evaluation of the Illumina MethylationEPIC BeadChip microarray for whole-genome DNA methylation profiling. Genome Biol. 2016;17(1):208.
37. Aryee MJ, Jaffe AE, Corrada-Bravo H, Ladd-Acosta C, Feinberg AP, Hansen KD, et al. Minfi: a flexible and comprehensive Bioconductor package for the analysis of Infinium DNA methylation microarrays. Bioinformatics. 2014;30(10):1363–9.
38. Fortin JP, Labbe A, Lemire M, Zanke BW, Hudson TJ, Fertig EJ, et al. Functional normalization of 450k methylation array data improves replication in large cancer studies. Genome Biol. 2014;15(12):503.
39. Maksimovic J, Gordon L, Oshlack A. Swan: subset-quantile within array normalization for illumina infinium HumanMethylation450 BeadChips. Genome Biol. 2012;13(6):R44.
40. Xu Z, Niu L, Li L, Taylor JA. Enmix: a novel background correction method for Illumina HumanMethylation450 BeadChip. Nucleic Acids Res. 2016;44(3):e20.
41. Xu Z, Langie SA, De Boever P, Taylor JA, Niu L. Relic: a novel dye-bias correction method for Illumina Methylation BeadChip. BMC Genomics. 2017;18(1):4.
42. Niu L, Xu Z, Taylor JA. Rcp: a novel probe design bias correction method for Illumina Methylation BeadChip. Bioinformatics. 2016;32(17):2659–63.
43. Kumanyika S, Tell GS, Shemanski L, Polak J, Savage PJ. Eating patterns of community-dwelling older adults: the Cardiovascular Health Study. Ann Epidemiol. 1994;4(5):404–15.
44. Nettleton JA, Schulze MB, Jiang R, Jenny NS, Burke GL, Jacobs DR Jr. A priori-defined dietary patterns and markers of cardiovascular disease risk in the Multi-Ethnic Study of Atherosclerosis (MESA). Am J Clin Nutr. 2008;88(1):185–94.
45. Del Gobbo LC, Kalantarian S, Imamura F, Lemaitre R, Siscovick DS, Psaty BM, et al. Contribution of Major Lifestyle Risk Factors for Incident Heart

Failure in Older Adults: The Cardiovascular Health Study. JACC Heart Fail. 2015;3(7):520–8.
46. Wang M, Li XS, Wang Z, de Oliveira Otto MC, Lemaitre RN, Fretts A, et al. Trimethylamine N-oxide is associated with long-term mortality risk: the multi-ethnic study of atherosclerosis. Eur Heart J. 2023;44(18):1608–18.
47. de Koning L, Chiuve SE, Fung TT, Willett WC, Rimm EB, Hu FB. Diet-quality scores and the risk of type 2 diabetes in men. Diabetes Care. 2011;34(5):1150–6.
48. Fung TT, Chiuve SE, McCullough ML, Rexrode KM, Logroscino G, Hu FB. Adherence to a DASH-style diet and risk of coronary heart disease and stroke in women. Arch Intern Med. 2008;168(7):713–20.
49. McCullough ML, Feskanich D, Stampfer MJ, Giovannucci EL, Rimm EB, Hu FB, et al. Diet quality and major chronic disease risk in men and women: moving toward improved dietary guidance. Am J Clin Nutr. 2002;76(6):1261–71.
50. Bertoni AG, Whitt-Glover MC, Chung H, Le KY, Barr RG, Mahesh M, et al. The association between physical activity and subclinical atherosclerosis: the Multi-Ethnic Study of Atherosclerosis. Am J Epidemiol. 2009;169(4):444–54.
51. Geffken DF, Cushman M, Burke GL, Polak JF, Sakkinen PA, Tracy RP. Association between physical activity and markers of inflammation in a healthy elderly population. Am J Epidemiol. 2001;153(3):242–50.
52. Inker LA, Schmid CH, Tighiouart H, Eckfeldt JH, Feldman HI, Greene T, et al. Estimating glomerular filtration rate from serum creatinine and cystatin C. N Engl J Med. 2012;367(1):20–9.
53. Houseman EA, Accomando WP, Koestler DC, Christensen BC, Marsit CJ, Nelson HH, et al. DNA methylation arrays as surrogate measures of cell mixture distribution. BMC Bioinformatics. 2012;13:86.
54. Keshawarz A, Bui H, Joehanes R, Ma J, Liu C, Huan T, et al. Expression quantitative trait methylation analysis elucidates gene regulatory effects of DNA methylation: the Framingham Heart Study. Sci Rep. 2023;13(1):12952.
55. Watanabe K, Taskesen E, van Bochoven A, Posthuma D. Functional mapping and annotation of genetic associations with FUMA. Nat Commun. 2017;8(1):1826.
56. Mootha VK, Lindgren CM, Eriksson KF, Subramanian A, Sihag S, Lehar J, et al. PGC-1alpha-responsive genes involved in oxidative phosphorylation are coordinately downregulated in human diabetes. Nat Genet. 2003;34(3):267–73.
57. Subramanian A, Tamayo P, Mootha VK, Mukherjee S, Ebert BL, Gillette MA, et al. Gene set enrichment analysis: a knowledge-based approach for interpreting genome-wide expression profiles. Proc Natl Acad Sci U S A. 2005;102(43):15545–50.
58. Hemani G, Zheng J, Elsworth B, Wade KH, Haberland V, Baird D, et al. The MR-Base platform supports systematic causal inference across the human phenome. Elife. 2018;30(7):e34408.
59. Ma J, Joehanes R, Liu C, Keshawarz A, Hwang SJ, Bui H, et al. Elucidating the genetic architecture of DNA methylation to identify promising molecular mechanisms of disease. Sci Rep. 2022;12(1):19564.
60. Genomes Project C, Auton A, Brooks LD, Durbin RM, Garrison EP, Kang HM, et al. A global reference for human genetic variation. Nature. 2015;526(7571):68–74.
61. Sanderson E, Glymour MM, Holmes MV, Kang H, Morrison J, Munafo MR, et al. Mendelian randomization. Nat Rev Methods Primers. 2022. https://doi.org/10.1038/s43586-021-00092-5.
62. Aragam KG, Jiang T, Goel A, Kanoni S, Wolford BN, Atri DS, et al. Discovery and systematic characterization of risk variants and genes for coronary artery disease in over a million participants. Nat Genet. 2022;54(12):1803–15.
63. Yoshimura K, Aoki H, Ikeda Y, Fujii K, Akiyama N, Furutani A, et al. Regression of abdominal aortic aneurysm by inhibition of c-Jun N-terminal kinase. Nat Med. 2005;11(12):1330–8.
64. Kaab S, Barth AS, Margerie D, Dugas M, Gebauer M, Zwermann L, et al. Global gene expression in human myocardium-oligonucleotide microarray analysis of regional diversity and transcriptional regulation in heart failure. J Mol Med (Berl). 2004;82(5):308–16.
65. Petretto E, Sarwar R, Grieve I, Lu H, Kumaran MK, Muckett PJ, et al. Integrated genomic approaches implicate osteoglycin (Ogn) in the regulation of left ventricular mass. Nat Genet. 2008;40(5):546–52.
66. Kohler S, Gargano M, Matentzoglu N, Carmody LC, Lewis-Smith D, Vasilevsky NA, et al. The Human Phenotype Ontology in 2021. Nucleic Acids Res. 2021;49(D1):D1207–17.
67. Fulcher JA, Hashimi ST, Levroney EL, Pang M, Gurney KB, Baum LG, et al. Galectin-1-matured human monocyte-derived dendritic cells have enhanced migration through extracellular matrix. J Immunol. 2006;177(1):216–26.
68. Iglesias-Carres L, Hughes MD, Steele CN, Ponder MA, Davy KP, Neilson AP. Use of dietary phytochemicals for inhibition of trimethylamine N-oxide formation. J Nutr Biochem. 2021;91:108600.
69. Donaldson SS, Whitaker SJ, Plowman PN, Link MP, Malpas JS. Stage I-II pediatric Hodgkin's disease: long-term follow-up demonstrates equivalent survival rates following different management schemes. J Clin Oncol. 1990;8(7):1128–37.
70. Atici AE, Crother TR, Noval Rivas M. Mitochondrial quality control in health and cardiovascular diseases. Front Cell Dev Biol. 2023;11:1290046.
71. Liu Y, Westerman KE, Ordovas JM, Lai C. Chapter 9 - Diet, DNA methylation, and cardiovascular disease2024.
72. Gonzalez-Castro TB, Tovilla-Zarate CA, Lopez-Narvaez ML, Juarez-Rojop IE, Calderon-Colmenero J, Sandoval JP, et al. Association between congenital heart disease and NKX2.5 gene polymorphisms: systematic review and meta-analysis. Biomark Med. 2020;14(18):1747–57.
73. Min JL, Hemani G, Hannon E, Dekkers KF, Castillo-Fernandez J, Luijk R, et al. Genomic and phenotypic insights from an atlas of genetic effects on DNA methylation. Nat Genet. 2021;53(9):1311–21.
74. Ueland PM, Holm PI, Hustad S. Betaine: a key modulator of one-carbon metabolism and homocysteine status. Clin Chem Lab Med. 2005;43(10):1069–75.
75. Sternbach S, West N, Singhal NK, Clements R, Basu S, Tripathi A, et al. The BHMT-betaine methylation pathway epigenetically modulates oligodendrocyte maturation. PLoS ONE. 2021;16(5):e0250486.
76. Chamberlain JA, Dugue PA, Bassett JK, Hodge AM, Brinkman MT, Joo JE, et al. Dietary intake of one-carbon metabolism nutrients and DNA methylation in peripheral blood. Am J Clin Nutr. 2018;108(3):611–21.
77. Zuo H, Svingen GF, Tell GS, Ueland PM, Vollset SE, Pedersen ER, et al. Plasma Concentrations and Dietary Intakes of Choline and Betaine in Association With Atrial Fibrillation Risk: Results From 3 Prospective Cohorts With Different Health Profiles. J Am Heart Assoc. 2018;7(8):e008190.
78. Abratte CM, Wang W, Li R, Axume J, Moriarty DJ, Caudill MA. Choline status is not a reliable indicator of moderate changes in dietary choline consumption in premenopausal women. J Nutr Biochem. 2009;20(1):62–9.
79. Lever M, George PM, Elmslie JL, Atkinson W, Slow S, Molyneux SL, et al. Betaine and secondary events in an acute coronary syndrome cohort. PLoS ONE. 2012;7(5):e37883.

Publisher's Note